

Dynamic Modeling of Limited Particle Coagulation in Emulsion Polymerization

M. J. J. MAYER,* J. MEULDIJK, and D. THOENES

Laboratory of Chemical Process Technology, Eindhoven University of Technology, P.O. Box 513, 5600 MB Eindhoven, The Netherlands

SYNOPSIS

In emulsion polymerization, a limited degree of particle coagulation may occur. Particle coagulation is caused by a loss of colloidal stabilization when the surface coverage of emulsifier on the particles drops below a critical value. It has been demonstrated experimentally in a previous article that the time scale for particle coagulation is small compared to the time scale for particle growth by polymerization and absorption of monomer. This indicates that the coagulation process can probably be described by von Smoluchowski kinetics. Based on this result, a comprehensive dynamic model for the simulation of limited particle coagulation in emulsion polymerization has been developed. It has been shown that there is a reasonable agreement between simulations with the dynamic model and experimental data (e.g., conversion time history, particle number, and particle size distribution). © 1996 John Wiley & Sons, Inc.

INTRODUCTION

During the batch emulsion polymerization of styrene with disproportionated rosin acid soap (DRAS) as emulsifier, the colloidal stability of the growing particles may be lost in many cases in that stage of the process in which the particles grow at the expense of the monomer droplets (interval 2). Meuldijk et al.¹ and Mayer et al.² have shown that the colloidal stability is lost when the fractional surface coverage of the growing particles with emulsifier falls below a critical value (θ_{crit}). It has also been shown that the time scale for limited particle coagulation is considerably smaller than the time scale for particle growth by polymerization and absorption of monomer. It is assumed that the coagulation process can be described with von Smoluchowski kinetics. In this article a dynamic model is reported for the simulation of limited particle coagulation in emulsion polymerization. The model simulations are compared with experimental results.

DYNAMIC MODELING OF EMULSION POLYMERIZATION

In the literature, a large number of articles have dealt with dynamic phenomena occurring during emulsion polymerization.³⁻¹⁴ More recently, Rawlings and Ray¹⁵ presented a dynamic model for emulsion polymerization in a single continuously operated stirred tank reactor (CSTR). This dynamic model comprises material balances, a radical population balance, the evolution of a particle size distribution, and micellar nucleation. The numerical technique used by Rawlings and Ray for solving the model equations was orthogonal collocation on finite elements. Besides the physical and chemical phenomena which have already been incorporated into the model developed by Rawlings and Ray, homogeneous particle formation and limited particle coagulation may play an important role in emulsion polymerization.^{2,16-18} However, to the best of our knowledge, no dynamic model has been presented that comprises all of the following: micellar and homogeneous nucleation, the evolution of a particle size distribution, a radical population balance, and limited particle coagulation.

To obtain a more general dynamic model for

* To whom correspondence should be addressed.

(continuous) emulsion polymerization, the model equations presented by Rawlings and Ray have been solved by a simple and straightforward first-order Euler method. This approach provides, besides its simplicity, the important advantage (beyond more sophisticated integration methods) that both the model and solving technique can be extended easily with other physical and chemical processes that may be important in emulsion polymerization (e.g., homogeneous nucleation and limited particle coagulation¹⁹). The set-up of the CSTR model is modular, so it can be applied for the simulation of, for example, a batch reactor and a series of CSTRs. The batch process can be simulated simply by setting the feed stream and the product stream of the CSTR to zero. The process in a series of CSTRs can be simulated by using the product stream of CSTR # j as a feed stream of CSTR #($j + 1$).

SIMULATION OF LIMITED PARTICLE COAGULATION WITH VON SMOLUCHOWSKI KINETICS

When, as a result of particle growth, the total particle surface becomes so large that the fractional surface coverage of emulsifier (θ) drops below the critical value (θ_{crit}), the latex particles will coagulate to such an extent that the critical surface coverage is reached again. The decrease of the total particle surface $\Delta A_{p,tot}$ as a result of coagulation is given by

$$\Delta A_{p,tot} = A_{p,tot}(\theta < \theta_{crit}) - \frac{(C_{E0} - C_{CMC})a_s N_{Av}}{\theta_{crit}} \quad (1)$$

where $A_{p,tot}(\theta < \theta_{crit})$, $C_{E,t}$, C_{CMC} , a_s , and N_{Av} , respectively, stand for the particle surface just before the coagulation step, the overall amount of emulsifier in the reactor at time t per volume unit of water, the critical micelle concentration, the surface of one emulsifier molecule adsorbed on the particles, and Avogadro's number. The second term in Eq. (1) stands for the critical particle surface below which coagulation occurs.

Von Smoluchowski²⁰ derived an equation for the collision frequency of particles from different size classes:

$$B(i, j) = f(\dot{\gamma}) N(i) N(j) [d_p(i) + d_p(j)]^3 \quad (2)$$

where $B(i, j)$ and $f(\dot{\gamma})$, respectively, stand for the number of collisions between particles in size class

i and size class j and a proportionality constant which depends on the shear rate. For a stirred tank, $\dot{\gamma}$ reflects the shear rate in the impeller zone. For the number of collisions between particles belonging to the same size class ($B(i, j)$), the following relation can be derived:

$$B(i, j) = f(\dot{\gamma}) N(i) (N(i) - 1) [2d_p(i)]^3 \quad (3)$$

With the assumption that $f(\dot{\gamma})$ is independent of the particle diameter, the total number of collisions in a latex with N_{tot} particle size classes is proportional to

$$K = \sum_{i=1}^{N_{tot}} \sum_{j=i+1}^{N_{tot}} [(d_p(i) + d_p(j))^3 N(i) N(j)] + \frac{1}{2} \sum_{i=1}^{N_{tot}} [(2d_p(i))^3 N(i) (N(i) - 1)] \quad (4)$$

The decrease of the particle surface as a result of coagulation of N_{coag} particles in a latex with N_{tot} particle size classes is equal to

$$\Delta A_{p,tot} = N_{coag} \pi \left(\left[\sum_{i=1}^{N_{tot}} d_p^2(i) f(i) \right] - \left[\frac{1}{2} \sum_{i=1}^{N_{tot}} \sum_{j=i+1}^{N_{tot}} d_p^2(i, j) f(i, j) + \frac{1}{2} \sum_{i=1}^{N_{tot}} d_p^2 f(i, j) \right] \right) \quad (5)$$

where

$$f(i) = \frac{\frac{1}{2} \left(\sum_{j=1}^{N_{tot}} [(d_p(i) + d_p(j))^3 N(i) N(j)] \right) - \frac{1}{2} (2d_p(i))^3 N(i)}{K} \quad (6)$$

$$f(i, j) = \frac{(d_p(i) + d_p(j))^3 N(i) N(j)}{K} \quad (7)$$

$$f(i, i) = \frac{(d_p(i) + d_p(i))^3 N(i) (N(i) - 1)}{K} \quad (8)$$

The first term on the right-hand side of Eq. (5) represents the surface of the coagulating particles. The second term on the right-hand side of Eq. (5) accounts for the particle surface created by coalescence of the coagulating particles. The overall number of particles that coagulates (N_{coag}) can be obtained by substitution of Eq. (5) into Eq. (1). The number

and size of the particles formed by coagulation followed by coalescence can be calculated from

$$N_{\text{coalesc}}(i, j) = \frac{1}{2} N_{\text{coag}} f(i, j) \quad (9)$$

$$d_p(i, j) = \left[\frac{6}{\pi} (v(i) + v(j)) \right]^{1/3} \quad (10)$$

where $v(i)$ and $v(j)$, respectively, stand for the volume of a particle in size class i and in size class j .

With a radical population balance over the discrete particle size distribution, as presented in a previous article,² the coagulation model, and the model equations presented by Rawlings and Ray, the time evolution of a particle size distribution as a result of particle growth by both absorption of monomer and limited coagulation can now be simulated. For this purpose, the model equations involving particle growth by absorption of monomer and polymerization and coagulation are solved simultaneously with small timesteps Δt . After each timestep, the discrete particle size distribution is actualized.

SOLUTION OF THE MODEL EQUATIONS

Figure 1 shows a simplified flow chart of the algorithm for the dynamic simulation of limited particle coagulation in (continuous) emulsion polymerization. Hereafter, each element of the flow chart is explained.

Element 1: The composition of the reaction mixture at time $t = 0$ and the operating conditions are defined.

Element 2: The monomer concentration in the water phase $C_{m,w}$, the amount of monomer in the monomer droplets C_{droplets} , and the monomer concentration in the particles $C_{M,p}$ are calculated through a mass balance for the monomer in the reactor and a thermodynamic relation for the equilibrium concentration of monomer in the particles and in the water phase.²¹ When the monomer droplets are absent, the value of $C_{M,w}$ and $C_{M,p}$ must be calculated iteratively from the monomer balance and the Morton equation.

Element 3: The size of the monomer swollen particles in each size class is calculated. The change of the total particle volume in each size class (i) during the time interval Δt follows directly from the polymerization rate $R_p(i)$.

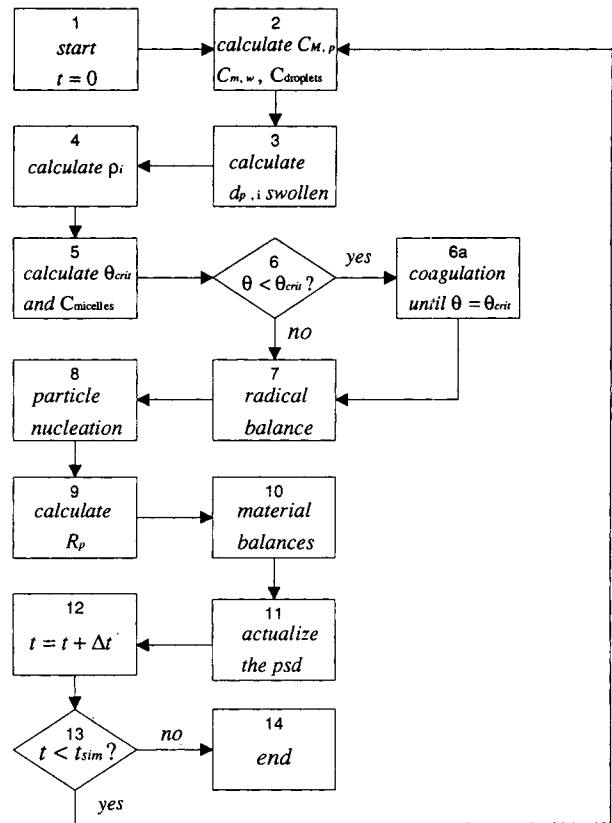


Figure 1 A simplified flow chart of the algorithm for the dynamic simulation of limited particle coagulation in (continuous) emulsion polymerization.

Element 4: Based on the initiator concentration in the water phase, the rate of radical formation ($\rho_i = 2f k_i C_{I,t}$) is calculated.

Element 5: The micelle concentration (C_{micelles}) is calculated through a material balance for the emulsifier in the reactor. If no micelles are present, the fractional surface coverage of emulsifier on the particles (θ) is calculated.

Element 6: If $\theta < \theta_{\text{crit}}$, then limited particle coagulation will occur.

Element 6a: Particle coagulation will occur until $\theta = \theta_{\text{crit}}$. The influence of limited particle coagulation on the particle size distribution is calculated through Eqs. (1) to (10). Each time limited particle coagulation occurs, the total number of particle size classes (N_{tot}) increases as follows:

$$N_{\text{tot}}(t + \Delta t) = N_{\text{tot}}(t) + \sum_{i=1}^{N_{\text{tot}}} \sum_{j=1}^{N_{\text{tot}}} (i \cdot j) \quad (11)$$

The increase of N_{tot} with the process time (t)

leads to such array sizes that the model equations can hardly be solved with the present computer technology. For this reason, a new grid of particle size classes is defined at each timestep Δt . The particle size distribution is calculated by a redistribution of the particles over the last defined grid. In this procedure, either surface- or volume-averaged diameters can be used, which means that an error in either the total particle volume or in the total particle surface is introduced. Therefore, it is necessary to track the overall error in the particle surface or particle volume during the dynamic simulation. Since a very large number of particle size classes (especially those with the largest particle diameters) contains a negligible number of particles, regridding can be avoided in many cases. The simulations presented in this article have been performed without the regrid procedure.

Element 7: The radical population balance over the discrete particle size distribution is solved iteratively. This is done by estimating the radical concentration in the water phase and calculating the time-averaged number of growing chains per particle (\bar{n}_i) for each particle size class. Subsequently, the overall radical balance is checked and, if necessary, the value of $C_{R,w}$ is adjusted. This procedure is repeated until the radical balance is valid within a desired accuracy. For the calculation of \bar{n}_i , the radical population balance is solved using a continuous fraction approximation.²² In case of particle nucleation, radical consumption by either micellar nucleation or homogeneous nucleation must be involved in the radical population balance.

Element 8: The rate of particle nucleation is calculated through an extended form of the relation proposed by Harada and Nomura²³ and a model for homogeneous nucleation.¹⁹ At each time interval Δt during which particle nucleation occurs, a new particle size class is generated.

Element 9: The total rate of polymerization R_p is calculated.

Element 10: In case of continuous reactor operation, the mass balances for the monomer, the emulsifier, the water, and the initiator are actualized.

Element 11: The particle size distribution is actualized. The influences of the feed stream and

the product stream on the particle number in each size class are taken into account.

Element 12: The desired process data, such as the total particle number, the polymerization rate, the particle size distribution, and the monomer conversion, are saved into a file.

Element 13: The process time is increased with a timestep Δt .

EXPERIMENTAL

The model calculations have been performed on a Silicon Graphics Power Challenge (16 150-MHz processors) supercomputer. For a characteristic timestep Δt of 1 s, the total relative integration error was less than 1%.

RESULTS

The influence of limited particle coagulation on the course of the particle number and the conversion as functions of time have been reported earlier for the batch emulsion polymerization of styrene.^{1,2,24} Mayer et al.^{2,24} have studied two different cases:

- Case 1, in which coagulation occurred as a result of a loss of electrostatic repulsion between the particles² ($\theta < \theta_{crit}$).
- Case 2, in which coagulation was excluded completely by feeding emulsifier into the reaction mixture after the nucleation period with such a rate that neither coagulation nor secondary nucleation occurred²⁴ ($\theta_{crit} \leq \theta \leq 1$).

For both cases, some major results have been summarized in Table I and Figure 2.

Table I Particle Number and Volume-Averaged Particle Size for a Batch Emulsion Polymerization of Styrene with DRAS as Emulsifier at 50°C

Case	$N_{product}$ ($10^{21}/m^3_{water}$)	$d_{p,vol}$ (nm)
1	4.3	57
2	7.7	47

$C_{K^*} = 0.14 \text{ kmol}/m^3_{water}$, $C_{M0} = 4.04 \text{ kmol}/m^3_{water}$, $C_{E0} = 0.095 \text{ kmol}/m^3_{water}$, $C_{I0} = 0.013 \text{ kmol}/m^3_{water}$. The value of θ_{crit} has been determined at 0.51.²

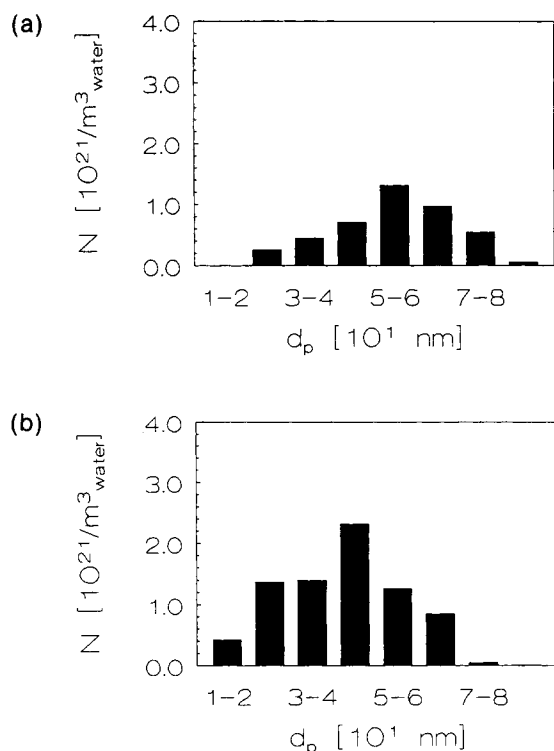


Figure 2 Particle size distributions of the product latex for the batch emulsion polymerizations of styrene with DRAS as emulsifier (a) with limited particle coagulation and (b) without limited particle coagulation.

To focus on the influence of limited particle coagulation on the particle size distribution and to exclude the stage of particle nucleation from the simulations, the following procedure has been applied to validate the coagulation model: From the particle size distribution of the batch experiment which is representative for case 2 [Table I and Fig 2(b)], the particle size distribution has been calculated at the point of time at which θ just falls below θ_{crit} for the first time. At this time t_{coag} , the coagulation process starts. The particle size distribution at t_{coag} has been calculated by integration of the monomer balance in opposite direction (i.e., from complete conversion to the conversion at t_{coag}). The polymerization rate in this balance has been calculated from a radical population balance over the particle size distribution.² Subsequently, both the evolution of the particle size distribution and the conversion time history have been simulated for $t > t_{\text{coag}}$ for the situation that coagulation is not suppressed (see case 1 in Table I).

Figure 3 shows the observed and simulated conversion time history and the particle number for

batch experiment with coagulation (see Table I). The physical and chemical parameters used for the model calculations have been summarized in Table II. In Figure 3 can be seen that there is a reasonable agreement between the model calculations and the experimental data, especially considering the relatively large influence of the experimentally determined value of θ_{crit} on the coagulation process. Note that the simulated conversion time history matches the experimental data and that there is hardly any influence of the particle number on the total polymerization rate, which is proportional to the slope of the curve. This is in accordance with the result that the effect of the decrease of the particle number on the polymerization rate is compensated for by the increase of the time-averaged number of growing chains per particle.² The large influence of θ_{crit} on the particle number in the product latex indicates a large influence of the cation concentration and the energy dissipation in the impeller region on the particle number. This has been observed experimentally.^{1,2} Figure 4 (see Mayer et al.²) shows the influence of the cation concentration on the particle number and θ_{crit} . In this figure two regions can be distinguished: a region in which the particle number in the product latex decreases as a function of the cation concentration in the recipe, and a region in which the particle number is independent of the cation concentration. In the first region, an increase of the cation concentration decreases the electrostatic repulsion between the latex particles. As a result, θ_{crit} increases, leading to a decrease of the

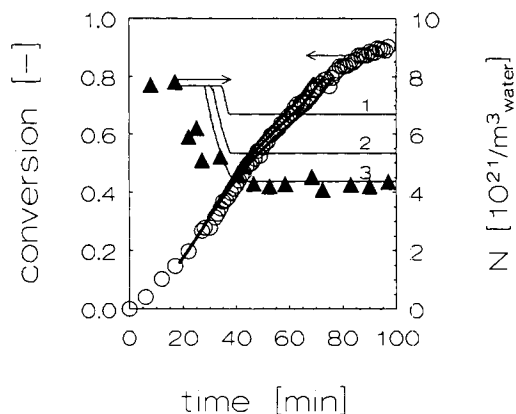


Figure 3 Batch emulsion polymerization of styrene with DRAS as emulsifier at 50°C. $C_{K^+} = 0.14$ kmol/ m^3_{water} , $C_{M0} = 4.1$ kmol/ m^3_{water} , $C_{E0} = 0.095$ kmol/ m^3_{water} , $C_{I0} = 0.013$. \circ conversion time history; \blacktriangle particle number as a function of conversion. 1,2,3: simulations with $\theta_{\text{crit}} = 0.46$, $\theta_{\text{crit}} = 0.51$, and $\theta_{\text{crit}} = 0.56$, respectively.

Table II Physical and Kinetic Parameters for the Emulsion Polymerization of Styrene with Sodium Persulphate as Initiator at 50°C

ρ_m (kg/m ³)	878	Weast ²⁵
ρ_p (kg/m ³)	1053	DeGraff et al. ²⁶
C_{M0} [kmol/m ³], X_m (-)	5.2, 0.43	Harada et al. ²³
k_p [m ³ /(kmol s)]	258	Rawlings and Ray ¹⁵
k_t [m ³ /(kmol s)]	$6.8 \cdot 10^7 \cdot \exp(-19X^{2.1})$	Hawkett et al. ²⁷
ρ_i [kmol/(m ³ s)]	$2fk_{i,t}$	Rawlings and Ray ¹⁵
f (-)	0.5	Rawlings and Ray ¹⁵
k_i (1/s) (50°C)	$1.6 \cdot 10^{-6}$	Rawlings and Ray ¹⁵
$(3D_m k_{trm})/k_p$ (m ²)	$6 \cdot 10^{-18}$	Hawkett et al. ²⁸
k_{tr} [m ² /(kmol s)]	$11k_{trm}$ (for $X \leq X_m$)	Mayer et al. ¹

particle number in the product latex. In the second region, electrostatic repulsion between the particles no longer contributes to the colloidal stability of the latex. In this situation the colloidal stability of the particles is completely determined by steric stabilization.

Figures 5(a) and 5(b), respectively, show the observed and simulated particle size distributions for a batch experiment with coagulation (see Table I, case 1). In figure 5 it can be seen that the particle size distribution of the product latex is simulated reasonably well by the dynamic model, except for the smallest particles.

Both simulations with the dynamic model and batch experiments demonstrate a considerable influence of θ_{crit} (i.e., the cation concentration on the

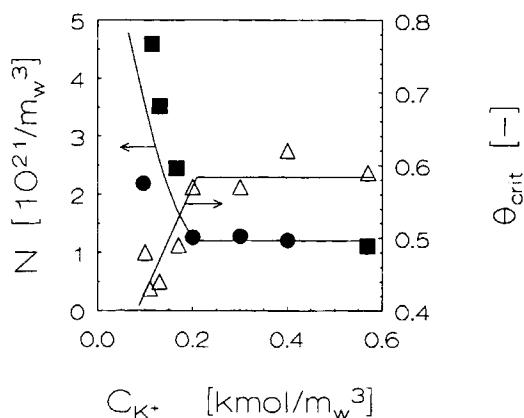


Figure 4 The particle number in the product latex and the value of θ_{crit} as a function of the cation concentration for the batch emulsion polymerization of styrene with DRAS as emulsifier at 50°C. $C_{M0} = 4.0$ kmol/m³_{water}, $C_{E0} = 0.07$ kmol/m³_{water}, $C_{I0} = 0.0125$ kmol/m³_{water}. ● ■ Particle number. Δ θ_{crit} .

particle number and the particle size distribution of the product latex). This shows that the dynamic model can be a useful tool for process optimization purposes. Using this model for process control will minimize the influence of small changes in the operating conditions on the product properties and so provide for constant product specifications.

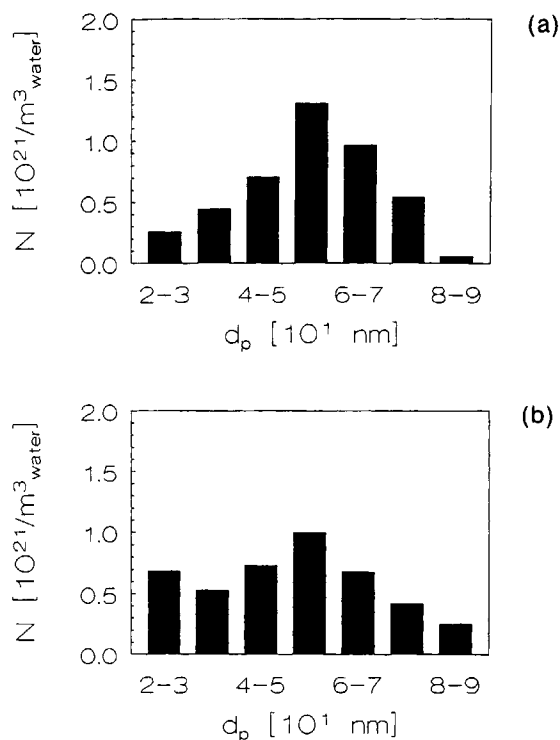


Figure 5 The observed (a) and simulated (b) particle size distributions for the batch experiment listed in Table I with limited particle coagulation. The coagulation process has been simulated with $\theta_{crit} = 0.56$. The physical and chemical parameters are summarized in Table II.

CRITICAL NOTE

The most important assumptions on which the coagulation model is based are as follows:

- The values of θ_{crit} and $f(\dot{\gamma})$ [see Eq. (2)] are independent of the particle size.
- The time scale for limited particle coagulation is considerably smaller than the time scale for particle growth by polymerization and absorption of monomer.

For emulsion polymerizations, in which these assumptions are not valid, more detailed modeling of the coagulation process is necessary.

CONCLUSIONS

- The experimental data on limited particle coagulation are predicted reasonably well by the dynamic model.
- The dynamic model can be a useful tool to predict the occurrence of limited particle coagulation and its influence on the polymerization process. In addition, it can be used for process control.
- Solution of the model equations with a simple first-order Euler integration method (resulting, among other things, in a discrete particle size distribution) has the advantage that the dynamic model can easily be extended with other chemical or physical processes that may be important in emulsion polymerization (e.g., limited particle coagulation).

The authors wish to thank DSM Research BV, Geleen, the Netherlands, for the financial support of this study and the students P. A. Knops, B. Kroes, J. H. A. Schoenmakers, R. H. G. Smeets, and J. A. M. Wijnen for their contribution to this work.

NOMENCLATURE

$A_{p,\text{tot}}$	Overall particle surface at complete conversion (m^2/m_w^3)
α_s	Surface that can be covered by one emulsifier molecule ($\text{m}^2/\text{molecule}$)
$B(i, j)$	Number of collisions between particles in size class i and size class j per unit of time ($1/\text{m}_w^3 \text{ s}$)

C_{CMC}	Critical micelle concentration (kmol/m_w^3)
C_{droplets}	Amount of monomer in the monomer droplets (kmol/m_w^3)
C_{EO}	Overall amount of emulsifier in the recipe (kmol/m_w^3)
C_{MO}	Overall amount of monomer in the recipe (kmol/m_w^3)
$C_{\text{M,p}}$	Monomer concentration in the particles (kmol/m^3)
$C_{\text{M,w}}$	Monomer concentration in the water phase (kmol/m_w^3)
$C_{r,w}$	Radical concentration in the water phase (kmol/m_w^3)
C_{tr}	Concentration of chain transfer agents (kmol/m^3)
D_m	Effective diffusivity of the small radicals (m^2/s)
$d_p(i)$	Particle diameter of size class i (m)
$f(\dot{\gamma})$	Proportionality constant in Eq. (2) [$\text{m}_w^3/(\text{m}_p^3 \text{ s})$]
$f(i)$	Fraction of particles in size class i that coagulates with respect to all coagulating particles N_{coag}
$f(i, j)$	Fraction of particles in size class i that coagulates with particles in size class j with respect to all coagulating particles N_{coag}
k_p	Propagation rate coefficient [$\text{m}^3/(\text{kmol s})$]
k_{tr}	Effective chain transfer rate coefficient [$\text{m}^3/(\text{kmol s})$]
k_{trm}	Chain transfer to monomer coefficient [$\text{m}^3/(\text{kmol s})$]
k_{trt}	Chain transfer to transfer agent coefficient [$\text{m}^3/(\text{kmol s})$]
N_{Av}	Avogadro's constant ($1/\text{kmol}$)
N_{coag}	Number of particles that coagulates ($1/\text{m}_w^3$)
$N(i)$	Number of particles in size class i ($1/\text{m}_w^3$)
\bar{n}_i	Average number of growing chains of particles in size class i (-)
R_p	Overall polymerization rate [$\text{kmol}/(\text{m}_w^3 \text{ s})$]
t	Reaction time (s)
t_{coag}	Reaction time at which $\theta < \theta_{\text{crit}}$ for the first time
$v(i)$	Volume of a particle in size class i (m^3)
X	conversion (-)

Greek Letters

ρ_i	Rate of radical formation by initiator decomposition [$\text{kmol}/(\text{m}_w^3 \text{ s})$]
----------	---

- θ Fractional surface coverage of emulsifier on the particles (—)
- θ_{crit} Fractional surface coverage of emulsifier on the particles below which colloidal stability is lost and limited particle coagulation occurs (—)

REFERENCES

- J. Meuldijk, G. F. M. Hoedemakers, M. J. J. Mayer, and D. Thoenes, in *Batch and Continuous Emulsion Polymerisation of Styrene: Recipes Not Obeying Simple Smith-Ewart Case II Kinetics*, K. H. Reichert and H. U. Moritz, Eds., Dechema Monographs, 127, VCH Verlagsgesellschaft, Weinheim, 1992, p. 417.
- M. J. J. Mayer, J. Meuldijk, and D. Thoenes, *J. Appl. Polym. Sci.*, **56**, 119 (1995).
- D. B. Gershberg and J. E. Longfield, 45th AIChE Meeting, New York, preprint #10, 1961.
- M. Nomura, M. Harada, K. Nakagawara, W. Eguchi, and S. Nagata, *J. Chem. Eng. Jap.*, **2**, 160 (1971).
- R. K. Greene, R. A. Gonzalez, and G. W. Poehlein, *ACS Symp. Ser.*, **24**, 341 (1976).
- V. A. Kirillov and W. H. Ray, *Chem. Eng. Sci.*, **33**, 1499 (1978).
- B. W. Brooks, H. W. Kropholler, and S. N. Purt, *Polymer*, **19**, 193 (1978).
- C. Kiparissides, J. F. MacGregor, and A. E. Hamielec, *J. Appl. Pol. Sci.*, **23**, 401 (1979).
- G. W. Poehlein, *ACS Symp. Ser.*, **104**, 1 (1979).
- F. J. Schork and W. H. Ray, *J. Appl. Polym. Sci.*, **34**, 1259 (1987).
- M. Nomura and M. Harada, *ACS Symp. Ser.*, **165**, 121 (1981).
- G. W. Poehlein, H. C. Lee, and N. Stubicar, in *Latex Production in Continuous Reactors*, K. H. Reichert and W. Geiseler, Eds., Hanser, Munich, 1983.
- E. E. Badder and B. W. Brooks, *Chem. Eng. Sci.*, **39**, 1499 (1984).
- T. O. Broadhead, A. E. Hamielec, and J. F. MacGregor, *Makromol. Chem. Suppl.*, **10/11**, 105 (1985).
- J. B. Rawlings and W. H. Ray, *Polym. Eng. Sci.*, **28**, 257 (1988).
- C. P. Roe, *Ind. Eng. Chem.*, **60**, 20 (1968).
- R. M. Fitch and C. H. Tsai, in *Polymer Colloids*, R. M. Fitch, Ed., Plenum Press, New York, 1971, p. 73.
- C. Kipparisides, J. F. MacGregor, and A. E. Hamielec, *Canad. J. Chem. Eng.*, **58**, 48 (1980).
- M. J. J. Mayer, *The Dynamics of Batch and Continuous Emulsion Polymerization*, Ph.D. thesis, Eindhoven University of Technology, May 1995.
- M. von Smoluchowski, *Z. Phys. Chem.*, **92**, 156 (1917).
- M. Morton, S. Kaizerman, and M. W. Altier, *J. Colloid Sci.*, **9**, 300 (1954).
- J. Ugelstad, P. C. Mörk, and J. O. Aassen, *J. Polym. Sci.*, **5**, 2281 (1967).
- M. Harada, M. Nomura, H. Kojima, W. Eguchi, and S. Nagata, *J. Appl. Polym. Sci.*, **16**, 811 (1972).
- M. J. J. Mayer, J. Meuldijk, and D. Thoenes, *J. Appl. Polym. Sci.*, to appear.
- R. C. Weast, *Handbook of Chemistry and Physics*, CRC Press, New York, 1977.
- A. W. DeGraff and G. W. Poehlein, *J. Polym. Sci.*, **9**, 1955 (1971).
- B. S. Hawkett, D. H. Napper, and R. G. Gilbert, *J. Chem. Soc. Faraday Trans. 1*, **77**, 2395 (1981).
- B. S. Hawkett, D. H. Napper, and R. H. Gilbert, *J. Chem. Soc. Faraday Trans. 1*, **76**, 1323 (1980).

Received November 30, 1994

Accepted June 5, 1995